

# Improving the Stability of Polylactic Acid Foams by Interfacially Adsorbed Particles

Juan Lobos,<sup>1</sup> Steven Iasella, Miguel A. Rodriguez-Perez,<sup>2</sup> Sachin S. Velankar<sup>1</sup>

<sup>1</sup> Chemical Engineering Department, University of Pittsburgh, Pittsburgh, Pennsylvania 15261, USA

<sup>2</sup> Cellular Materials Laboratory (CellMat), Condensed Matter Physics Department, University of Valladolid, Valladolid 47011, Spain

**Polymers such as poly(lactic acid) (PLA), which have poor melt strength, are difficult to foam due to severe cell coalescence during foaming. We show that addition of a few percent of polytetrafluoroethylene (PTFE) particles can stabilize PLA foams against bubble coalescence and collapse. The particles and a chemical blowing agent, were dispersed into the PLA by extrusion, and then foamed by heating. The PTFE-containing foams remained stable even when the foams were held under molten conditions for extended periods. Foam stability is attributed to an interfacial mechanism: due to their low surface energy, the PTFE particles adsorb on the inner surface of the foam bubbles at a high surface coverage, and endow the bubbles with an interfacial “shell” that prevents coalescence. This mechanism resembles the particle-stabilization of Pickering emulsions in oil/water systems. Particle adsorption at the interface is a necessary condition for using this approach, and hence this approach is most likely to be successful if the particles have a low surface energy and the polymer has a high surface tension. The approach of using interfacially adsorbed particles can be broadly generalized, and offers the opportunity of foaming various polymers with low melt strength, or for expanding the processing window within which foaming can be conducted. POLYM. ENG. SCI., 00:000–000, 2015. © 2015 Society of Plastics Engineers**

## INTRODUCTION

Poly(lactic acid) (PLA) is a biocompatible, environmentally friendly, biodegradable thermoplastic polymer manufactured from renewable raw materials. It has gained popularity for general use applications, especially single use packaging and consumer goods [1, 2]. Some of these applications, notably insulating packaging, would benefit from foamed PLA. However, it is difficult to foam PLA because its poor melt strength leads to massive cell coalescence or even foam collapse [3]. Moreover its susceptibility to molecular weight degradation by thermal or hydrolytic chain scission worsens the problem of poor melt strength [4]. Poor melt strength is not unique to PLA;

most notably linear polypropylene (PP) is notoriously difficult to foam [5, 6]. The problems of cell coalescence are compounded when foaming is to be combined with slow-cooling processes, such as rotomolding, which require the foam to stay under melt conditions for long periods.

Various approaches have been considered to improve the melt strength of PLA. One approach is chemical modification to increase the molecular weight and long chain branching [7, 8]. Another approach of ionic modification of PLA to induce physical crosslinking would likely have the same effect [9, 10]. Nanofillers have also been used to improve foaming characteristics [11–15], and some of the effect may be attributable to a rheological modification induced by the nanofiller. In this research we take a very different approach to improve stability of PLA foams. Similar to previous research [11–15], we add particles to the PLA, but in our case, the particles are intended to stabilize the foam structure under molten conditions by the mechanism of interfacial immobilization.

We start with the observation that although good melt strength is regarded as one of the key requirements for foaming thermoplastics, stable foams can be realized even from materials with no melt strength at all. The most familiar example is foams realized by agitating a water-surfactant mixture. In such cases, foam stability is attributable not to the bulk viscoelasticity of the cell walls, but instead to the interfacial viscoelasticity of the air/liquid interface. The interfacial phenomena include Marangoni stresses, Gibbs elasticity, and complex interfacial properties such as an interfacial shear viscosity or shear modulus [16, 17]. While surfactant stabilization is most familiar in aqueous foams, non-aqueous systems can also be stabilized using more specialized surfactants. Indeed polyurethane foam formulations typically include surfactants to stabilize foams temporarily, prior to polymerization and crosslinking within the cell walls.

Interfacial stabilization can also be achieved by particles—a phenomenon well-studied in aqueous foams [18–23]. The essential mechanism is that partially hydrophobic particles adsorb almost irreversibly at the air/water interface: such particles can then prevent coalescence. This same mechanism can be transplanted to polymeric systems as illustrated in Fig. 1. Fig. 1a illustrates a partially wettable particle, i.e., one that can adsorb at the free surface of the molten polymer making a certain contact angle  $\theta$ . Partial wettability means that  $\theta > 0$ , which typically corresponds to the surface energy of the particle being smaller than the surface tension of the molten polymer. In this case, if the particles adsorb at the interface at a sufficiently high coverage (Fig. 1b and c), the bubbles can become endowed with a mechanically robust shell which can prevent bubble coalescence and stabilize the foam.

Correspondence to: S.S. Velankar; e-mail: velankar@pitt.edu

Contract grant sponsor: NSF-CMMI; contract grant number: 1252850; contract grant sponsor: MINECO; contract grant number: MAT 2012-34901; contract grant sponsor: Junta of Castile and Leon; contract grant number: VA035U13.

Juan Lobos is currently at University of Yachay, San Miguel de Urcuqui 100119, Ecuador.

Additional Supporting Information may be found in the online version of this article.

DOI 10.1002/pen.24185

Published online in Wiley Online Library (wileyonlinelibrary.com).

© 2015 Society of Plastics Engineers

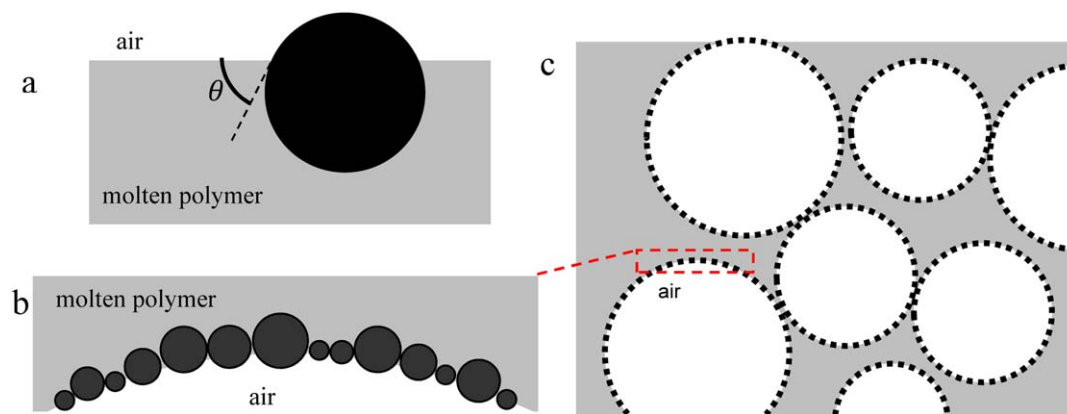


FIG. 1. (a) A particle with surface energy lower than the polymer can be adsorbed at the interface between polymer and air making a contact angle of  $\theta$ . With sufficient adsorption, particles can endow cells with a shell (b), which protects against coalescence to create a stable foam (c).

In a previous article, we tested proof-of-principle of this idea [24]. We examined the effect of adding 5 wt% polytetrafluoroethylene (PTFE) particles to three different polymers: polyisobutylene (PIB), polydimethylsiloxane (PDMS), and polystyrene (PS) of very low molecular weight. All three polymers were selected purely for experimental convenience: specifically, the PIB and PDMS were viscous liquids at room temperature, whereas the PS was a viscous liquid at roughly 85°C. Therefore in all three cases, particles could be dispersed into the polymer by hand-mixing with a spatula without needing polymer processing equipment. In all cases, the particles and a chemical blowing agent (CBA) were mixed into the polymer, and the mixtures were heated to decompose the CBA and nucleate bubbles. Analogous foaming experiments were conducted on all three polymers without PTFE particles.

Of the six samples, the following four showed complete collapse of their foam: all three polymers without PTFE particles, and the (PDMS + PTFE). In these samples, the nucleated bubbles rose to the surface and escaped, and not a single bubble survived after the decomposition of the CBA was completed. Two samples however showed completely different behavior: in the (PIB + PTFE) and (PS + PTFE), the bubbles rose to the surface but did not escape, and formed highly stable foams. It is noteworthy that both these polymers gave stable foams even though they were Newtonian liquids with no melt strength at all. Moreover, the PIB even remains liquid at room temperature, but nonetheless, the (PIB + PTFE) foam did not collapse even over one year.

This behavior can be understood in terms of the differing surface tension and wetting characteristics of the three polymers toward PTFE particles. The surface tension of the liquid PDMS was less than of the PTFE particles, and hence the particles were fully wetted by the PDMS. Thus PDMS foams collapsed completely since the particles stayed in the bulk and did not induce interfacial stabilization. In contrast, the surface tension of the liquid PIB or PS was more than of the PTFE particles. Hence the particles were only partially wetted by the PIB or by the PS, and hence adsorbed at the bubble surfaces, thus preventing bubble coalescence and stabilizing the foams. Direct confirmation of particle adsorption was possible in the case of PS foams since PS is solid at room temperature. Thus the bubble surfaces could be imaged by scanning electron microscopy (SEM), and indeed the inner surface was found to be completely covered by PTFE particles. In summary, our previous article

showed that interfacial stabilization is, at least in principle, a viable method to foam polymers with low melt strength.

However, this proof-of-principle did not prove practical viability since that research suffered from some important deficiencies. First, as noted above, for experimental convenience, the research employed polymers that were liquid at room temperature or at a fairly low temperature (for the PS). Thus these materials are not typical thermoplastics. Second, the sample preparation was quite dissimilar from commercial foaming operations. Specifically, due to the low viscosity, the nucleated bubbles rose upwards due to buoyancy. This bubble rise may have aided particle adsorption on the interface—an effect that is not expected in typical thermoplastic foaming where buoyancy effects are weak. Finally, due to the bubbles rising upwards, the eventual structure of the sample consisted of a “head” of foam floating atop a larger pool of unfoamed polymer. To illustrate this, a typical image of the final stable foam is reproduced in the Electronic Supporting Information, Fig. S1. This too is not typical of conventional thermoplastic foaming in which the entire sample must be foamed homogeneously. In summary, even though the idea of particle stabilization of polymer foams has been validated, our previous research is not representative of materials and processes in the foaming industry.

Accordingly, the goal of this article is to test whether particle stabilization is a viable approach for conventional thermoplastics foamed using a conventional foaming operation (free foaming using a CBA). Using linear PLA as a representative example of a low melt strength polymer, we show that interfacial stabilization of the foam is indeed possible, and the foams can be kept under molten conditions for extended periods without collapse. We also examine the mechanism by which the particles adsorb at the interface at sufficiently high coverage to prevent coalescence. We conclude with some comments on whether this approach to foam stabilization may be useful with other thermoplastic polymers with low melt strength.

## EXPERIMENTAL

### Materials

An injection molding grade PLA, Ingeo 3251D (NatureWorks LLC) with a melt flow index of 80g/10min at 210°C and 2.16 kg was used in this research. We have deliberately chosen a high melt flow grade for experiments because the low viscosity

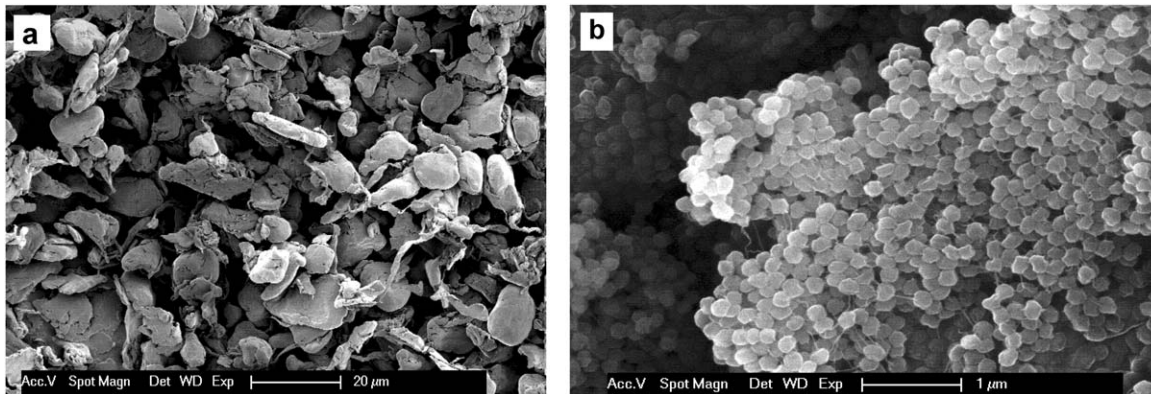


FIG. 2. SEM images of the (a) TF-9205 particles and (b) Zonyl MP1600 particles.

makes this resin especially unsuitable for foaming. The surface energy of the PLA,  $41\text{mN/m}^2$ , was measured by Otsuka [25].

Two different types of PTFE particles were used in this research, and their SEM images are shown in Fig. 2. The first was Dyneon PTFE TF 9205, the same as used in our previous article [20]. These particles are highly irregular in shape with a typical size of 5–15  $\mu\text{m}$ . The second was DuPont Zonyl MP 1600N with a primary particle size of 0.2  $\mu\text{m}$ . PTFE has a reported surface energy of 22.5  $\text{mN/m}$ , measured by Wu [26]. This is significantly lower than of the PLA, as required by the mechanism postulated in Fig. 1.

Azodicarbonamide (Porofor ADC/M-C1, produced by Lanxess), with an average particle size 3.9  $\mu\text{m}$  quoted by the supplier, was used as CBA at a 5 wt% loading. This is an exothermic blowing agent releasing mainly nitrogen. Being exothermic, its decomposition tends to raise the temperature of the foaming system, and hence also tends to exacerbate bubble coalescence.

#### Blending

The polymers were mixed with the azodicarbonamide and the PTFE particles in a twin-screw extruder (Collin Teach-line ZK 25T) in two successive passes at 150°C temperature. This blending temperature is substantially lower than the decomposition temperature of the foaming agent quoted by the manufacturer (210°C). The various compositions examined are listed in Table 1. Note that the density of PTFE ( $\sim 2000\text{ kg/m}^3$ ) is significantly higher than that of PLA ( $1300\text{ kg/m}^3$ ) and hence the PTFE loading of 5 wt% used in most of the experiments corresponds to roughly 3% by volume.

#### Foaming

The pellets were dried in a vacuum oven at 55°C for 24 h prior to foaming to reduce hydrolytic degradation. An aluminum

mold with four independent cylindrical cavities 0.75 inch (19 mm) in height and 0.75 inch in diameter was used to make four samples simultaneously. Each cavity was sealed with a Viton O-ring to prevent gas or polymer from leaking as the pressure rose with the decomposition of the azodicarbonamide. In each experiment, the four cavities were filled with weighed amounts of the four samples (in the form of pellets), and sealed. The mold was placed in the center of a platen press heated at 200°C for various times, and then allowed to cool on a metal surface at room temperature for 30 minutes before removing the foam cylinders. For short duration heating experiments to examine the initial stages of foam growth, faster cooling was desired. In these cases, the mold was quenched in water immediately after removing from the press. Incidentally note that our foaming temperature of 200°C is lower than the 210°C specified by the supplier of the CBA. Nevertheless, we were able to get adequate foaming at this temperature.

Most of the experiments were conducted with 1.5 g of polymer loaded into each mold cavity. Assuming complete filling, this corresponds to a nominal foam density of  $276\text{ kg/m}^3$ , although below we will present densities that were actually measured (see below). Additional experiments were conducted with 1 g or 2 g of polymer per cavity and the results were essentially identical to those noted here.

#### Characterization

The density of each cylindrical foam sample was measured using hydrostatic weighing in ethanol. The samples were then cut diametrically and photographed with a camera Canon EOS350D. SEM images were also recorded (see below). Optical and SEM images were processed and analyzed using the software ImageJ [27, 28] to obtain the average value of the cell diameter and the cell size distribution. The images selected for analysis had a resolution such that 60-100 cells were visible and the smallest cells were at least 10 pixels across. Corrections specified in the ASTM standard D3576 were applied to obtain the cell size for a 3D distribution of cells from a plane image [28]. Cell density was calculated using [29]:

$$N = \frac{6}{\pi \langle D^3 \rangle} \left( 1 - \frac{\rho_f}{\rho_s} \right) \quad (1)$$

TABLE 1. Samples compositions (all weight %).

Sample	PLA	TF9205	MP1600N	ADC/M-C1
PLA	95%	–	–	5%
PLA + 5TF	90%	5%	–	5%
PLA + 5Zonyl	90%	–	5%	5%
PLA + 10Zonyl	85%	–	10%	5%

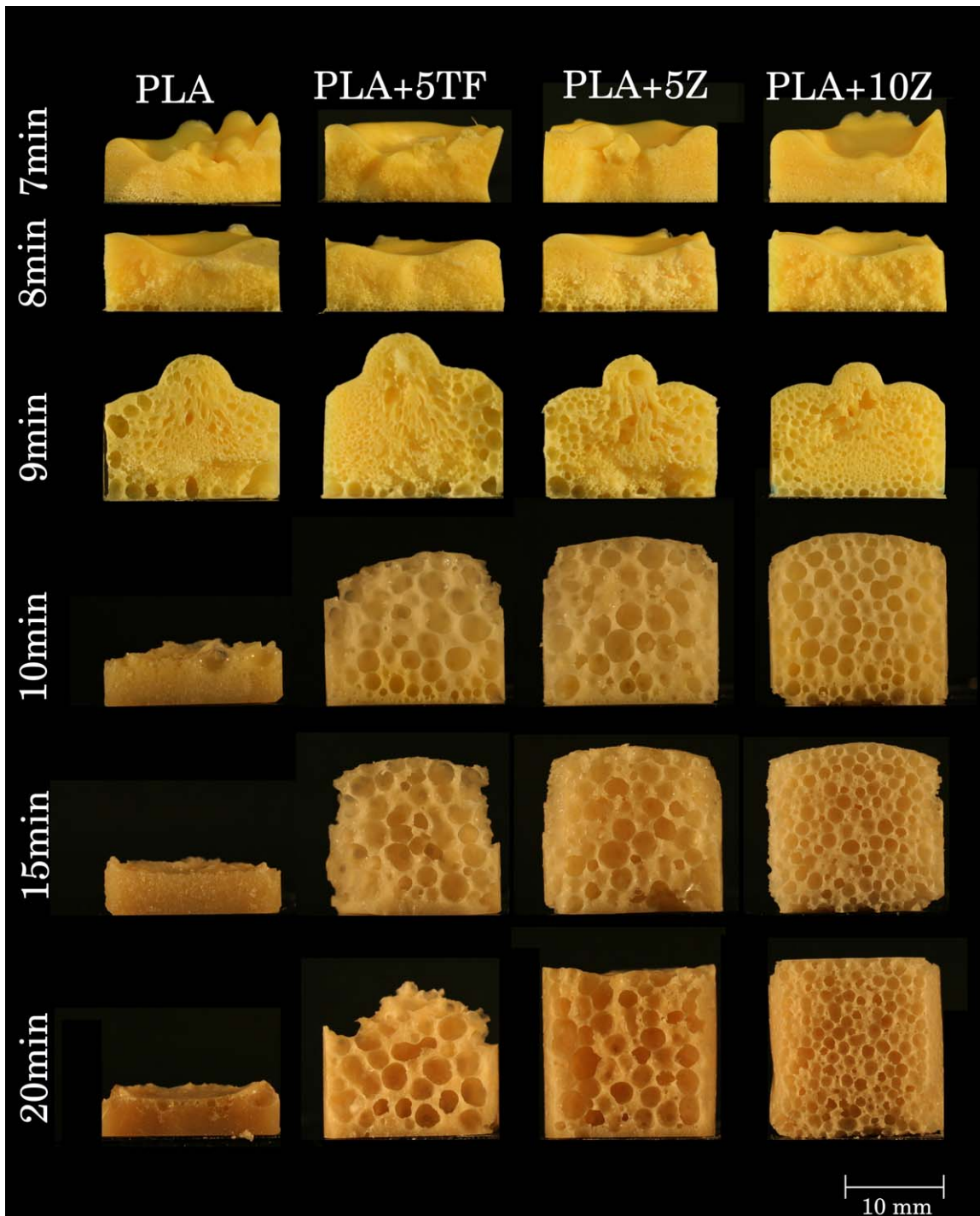


FIG. 3. Photographs of cross-sections of samples with 1.5 g of pellets, nominal density  $276 \text{ kg/m}^3$ . [Color figure can be viewed in the online issue, which is available at [wileyonlinelibrary.com](http://wileyonlinelibrary.com).]

where  $D$  is cell diameter and  $\pi\langle D^3 \rangle / 6$  represents the mean volume of a cell,  $\rho$  is the density of the foam, and  $\rho_s$  is the density of the solid pellets, measured in the same way as the foams.

Particle adsorption on the inner surface of the foam cells was observed by SEM (JEOL JSM6510) with the possibility to conduct elemental analysis (Oxford INCA EDS) to distinguish between PTFE particles and residue from the decomposition of azodicarbonamide during foaming.

## RESULTS AND DISCUSSION

### *Effect of Particle Type and Loading*

Figure 3 shows images of cross-sections of PLA foams obtained by loading 1.5 gram pellets into the molds. The samples had a skin which is visible in some of the images, e.g., bottom right image of Fig. 3, when the sample was not imaged exactly diametrically. Samples extracted prior to 6 minutes of

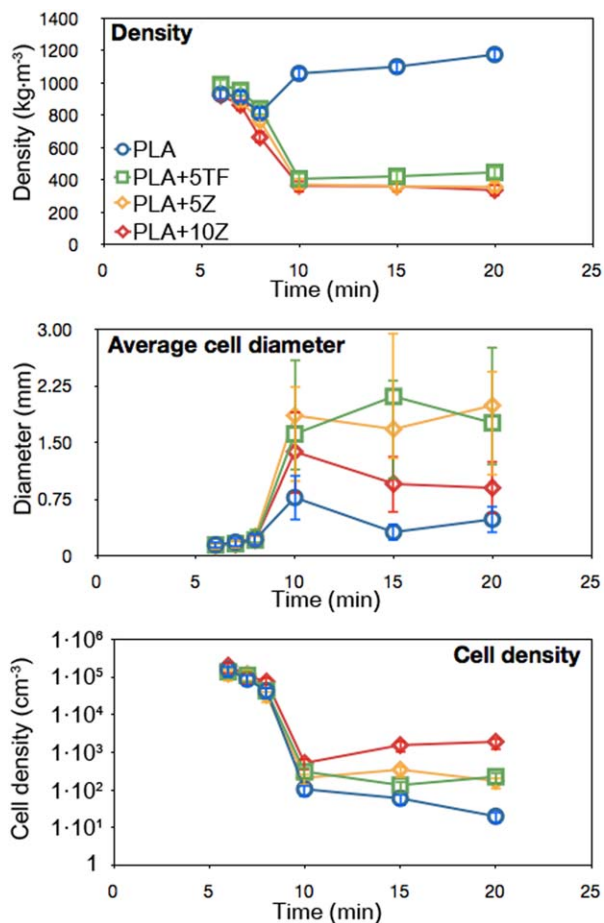


FIG. 4. Quantification of the PLA foams of Fig. 3. [Color figure can be viewed in the online issue, which is available at [wileyonlinelibrary.com](http://wileyonlinelibrary.com).]

heating time showed a significant number of unmelted pellets. At 7 minutes, much of the sample appears melted, although the top surface (farthest from the heated mold surface) still shows some incompletely melted pellets. Simultaneously, small nucleated bubbles appear, and SEM images (not shown) show a typical bubble size in the 140–180  $\mu\text{m}$  range. By 8 minutes, melting is complete, with the bubbles being  $\sim 250 \mu\text{m}$ , with the hottest portions of the samples (in contact with the bottom and sides of the mold) showing much larger bubbles. Subsequent foam rise is rapid, but the left column shows that for the particle-free PLA, collapse is equally rapid, and a stable foam is not formed. This is not surprising: PLA typically has poor foamability, and this specific grade with a high melt index (low viscosity) is especially unsuitable for foaming. In sharp contrast, all three of the particle-containing PLAs show stable foams, even when the foam is held under molten conditions for 20 minutes (i.e., 11 minutes past the initial foam rise) and when the samples are cooled slowly. Additional noteworthy features that are qualitatively evident from Fig. 3 are as follows. First, both PLA-5TF and PLA-5Z samples show some gravitational drainage as evident from the formation of a dense, bubble free layer at the bottom after 10 minutes under molten conditions. The PLA-10Z sample does not show such a drained layer; the cells appear uniform in size throughout the height as well as cross-section of the sample. Second, all three samples show a sharp increase in cell size between 8 and 10 minutes with only

modest changes at longer times. Finally, the PLA-10Z sample has smaller cell sizes at long times as compared to PLA-5Z.

Figure 4 quantifies the results of Fig. 3 by plotting the measured density, the average cell size, and the average cell density for the various foams. For the particle-free PLA, the density (Fig. 4a) reduces slightly after about 9 minutes of heating (when the CBA decomposition occurs), but then rises sharply as the

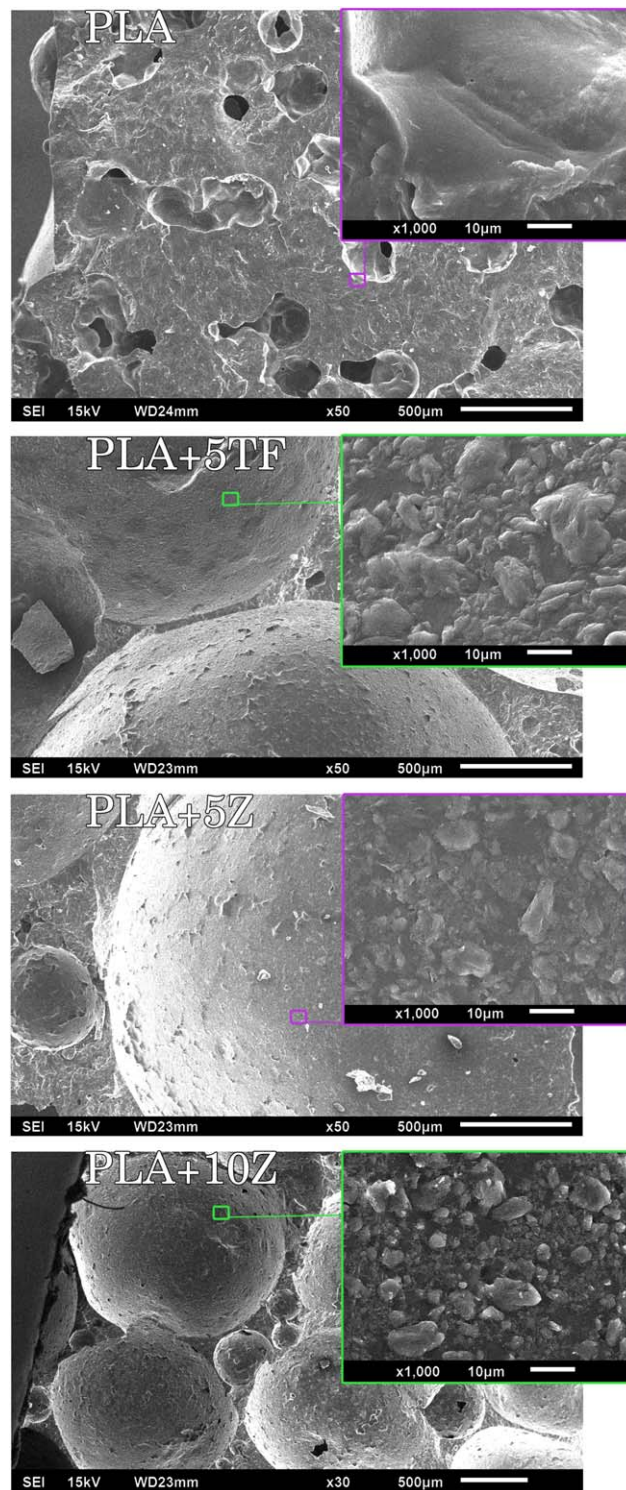


FIG. 5. SEM images of the cells of the PLA foams without and with PTFE particles, heated for 15 min.

foam collapses. Beyond 10 minutes, the density is not significantly different from that of unfoamed PLA. All three particle-containing foams show a decrease in density up to 10 minutes, and the density remains low although for the PLA + 5TF foam, the density rises slightly at long times. Figure 4b quantifies the changes in mean cell size, and 4c uses *Eq. 1* to calculate cell density. As was already qualitatively evident from Fig. 3, the PLA + 10Z samples have the smallest cell sizes and the highest cell density. We caution that although cell size and cell density data have been included for the particle-free foam, these data are not very meaningful: in particular, at long times (over 10 minutes), a small mean cell size is reported in Fig. 4b due to the few small bubbles remaining in the sample, whereas in reality this sample is almost completely collapsed.

Incidentally, experiments have been conducted for even longer durations under molten conditions, and the particle-containing foams do not collapse. However for times longer than 30 minutes, it is no longer possible to recover the foams intact from the molds because they become too brittle, presumably due to thermal degradation of the polymer, i.e., the foams are more stable than the polymer itself.

Finally, SEM imaging was conducted on foams extracted after 15 minutes under molten conditions to verify that the foam stabilization is specifically attributable to the interfacial adsorption of the particles. Figure 5 shows SEM images of the inner surface of the bubbles of all four foams at low magnification (on the scale of the bubbles) and at high magnification (on the scale of the particles). An even clearer comparison between the two particle types is shown in Electronic Supporting Information, Fig. S2. In all particle-containing foams, the inner surface is heavily covered with particles suggesting that interfacial adsorption is indeed responsible for foam stability. In contrast, the topmost image in Fig. 5 shows the collapsed particle-free foam. In this case, the internal surface of the bubble appears smooth suggesting that any possible residue from the decomposition of the CBA does not adsorb at the air/polymer interface.

#### Mechanism of Stabilization

The results of Figs. 3–5 show that interfacial adsorption of particles is an effective means of preventing foam collapse due to cell coalescence. Yet, it raises questions about the mechanism by which the particles reach the surface of the bubbles to such a high coverage. As detailed in the Introduction, the polymers used in our previous research [24] had very low viscosity, and during foaming, the bubbles rose to the top due to buoyancy. Thus, the sample as a whole was not foamed; instead, as shown in the Supporting Figure S1, a top layer of foam rested on a lower layer of liquid, analogous to froth on beer. In contrast, the foams of Fig. 3 are completely different, and more representative of standard thermoplastic foaming. Previously we had speculated that collisions between particles and the rising bubbles were the likely mechanism for particle adsorption. In contrast, buoyancy effects are negligible in Fig. 3 due to the high viscosity of the melt. Clearly, bubble rise does not contribute to particle adsorption, and some other mechanism must be responsible for the high surface coverage of particles. To elucidate the mechanism, additional SEM imaging was conducted as a function of time, i.e., for the samples of Fig. 3. The SEM images for the PLA+5Z sample at various foaming times are shown in

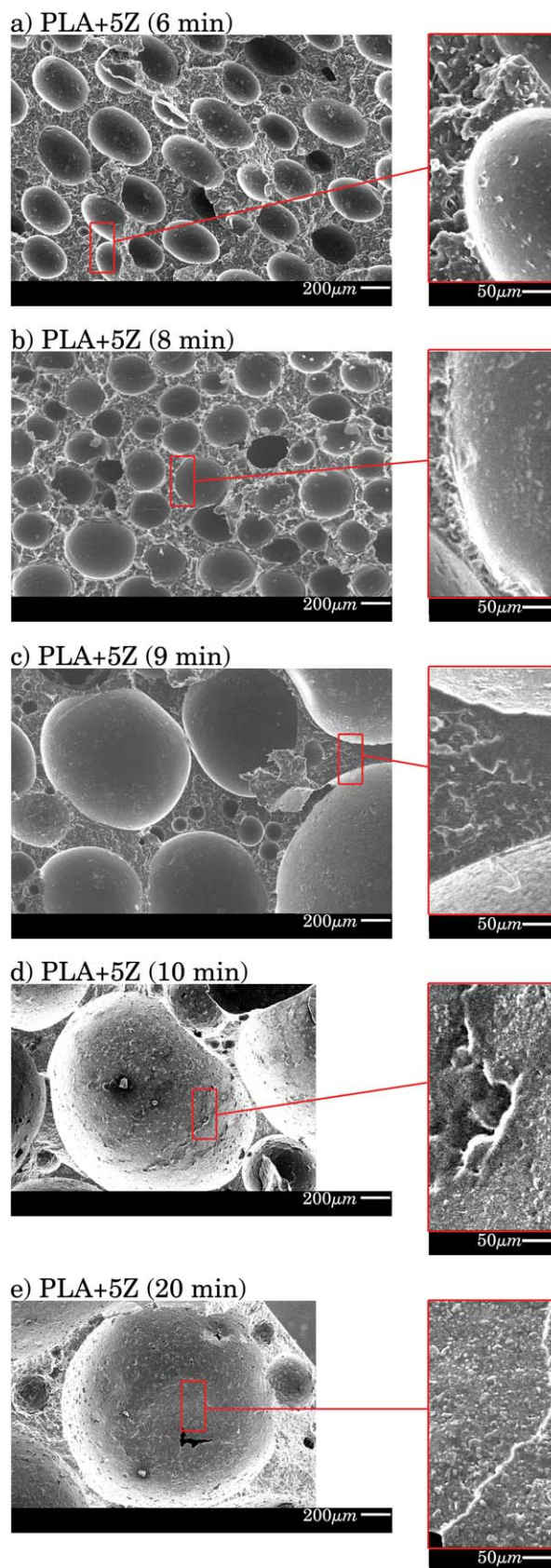


FIG. 6. SEM images of the cells of the PLA+5Z heated for various times.

TABLE 2. Properties of polyolefins used.

Sample	Supplier grade	MFI (g/10 min)
LDPE	Repsol Quimica	4 (190°C/2.16 kg)
Polypropylene	Braskem R7021-50RNA	50 (230°C/2.16 kg)
Polyolefin elastomer	Dow Versify 4301	25 (230°C/2.16 kg)

Fig. 6. Figure 6a and b show the cellular structure at short times when bubble nucleation has just started, and the cells are  $\sim 200$   $\mu\text{m}$  in size. It is noteworthy that particles are already visible on the surface of the bubbles, however, the surface coverage of the particles is low. Figure 6c shows the same sample after 9 minutes of heating. A bidisperse population of bubbles is evident with some of the bubbles being  $\sim 200$   $\mu\text{m}$  (same as at 8 minutes), and some being over 600  $\mu\text{m}$ . The larger bubbles appear to have a higher coverage of particles, although the coverage is still far short of complete. At 10 minutes, the small bubbles have mostly vanished, but the remaining bubbles are heavily covered by particles. At this stage, there remain some patches that have little or no particles adsorbed. Finally at 15 minutes, there is no significant change in the bubble size as compared to the sample at 10 minutes. However the particle-free patches are completely healed leaving a surface tightly covered with particles. These time-resolved SEM studies establish that there are two simultaneous and dramatic changes between 8 and 10 minutes: a sharp increase in particle coverage, which coincides with a sharp increase in bubble size due to coalescence.

The time evolution of foam structure for the PLA + 5TF samples was found to be similar to the PLA + 5Z sample. The corresponding series of images is shown in the Electronic Supporting Information (Fig. S3) and in that case as well, the increase in bubble size coincides with an increase in particle surface coverage. We have also prepared PLA foams with both particle types, but either 1 g or 2 g sample in each foaming chamber (corresponding to nominal densities of 184 and 368  $\text{kg}/\text{m}^3$  respectively). The visual appearance of the samples with increasing foaming time (published previously [30]) is identical to Fig. 3 although we have not conducted SEM studies with the same time-resolution as Fig. 6. Experiments using PS (instead of PLA) as the polymer gave similar results as well. These were published previously [30] and are reproduced in the Electronic Supporting Information Fig. S4. Once again, early during the foaming process, the surface coverage is low and the bubbles are small, whereas late in the process, the bubbles are much larger whereas the surface is nearly completely covered with particles. Collectively these observations suggest the following picture. Early during the decomposition of the blowing agent, while the bubbles are very small, the particles adsorb on the interface of the bubbles. Indeed it is possible that—given the low surface energy of the particles—the bubbles may nucleate on the particles. As the bubbles grow and impinge upon each other, they coalesce rapidly due to the poor melt strength of the polymer. We hypothesize that during this initial stage, the coalescence of particle-containing foams is not significantly different from those of the particle-free foams, i.e., the particles have little or no effect on bubble stability. However as the average bubble diameter increases, the total bubble area reduces, which

in turn has the effect of concentrating the particles on the surface, i.e. raising their surface coverage. Surface coverage may also increase as any particles that are not already on the surface diffuse to the surface with time. When the surface coverage is sufficiently high, the bubbles are now endowed with a shell of particles and subsequent coalescence slows down, i.e., coalescence is a self-limiting process.

While the particles used in this study are not necessarily spherical, in the case of spherical particles, one may readily describe the self-limiting state by the equation:

$$(\text{cell number density}) \times \langle \pi D^2 \rangle = (\text{particle number density}) \times \langle \pi R_p^2 \rangle \quad (2)$$

where  $R$  is the particle radius. Here the left hand side corresponds to the area of the bubbles per unit volume, whereas the right hand side is the cross-sectional area of the particles per unit volume. This equation assumes that all the particles adsorb on the bubble surfaces, and that the self-limiting state has full surface coverage. This equation immediately suggests that the cell size would decrease with increasing particle loading (i.e., increasing particle number density), and with decreasing particle size. The first trend is consistent with Figs. 3 and 4: PLA + 10Z has cell sizes that are almost 1.8 times smaller than PLA + 5Z. The second trend is also consistent with experiments: the cells of PLA + 5Z are substantially smaller than those of PLA + 5TF even though the particle loading is the same. This may be attributable to the smaller size of the Zonyl particles, and therefore a higher effective surface area at the same weight loading.

Incidentally it must be noted that in the case of the TF9205 particles, the typical size of the particles visible on the interface (Fig. 5a) is in the 5–15  $\mu\text{m}$  range, and not very different from what is apparent in Fig. 2. This suggests that the particles are well-dispersed prior to foaming. In contrast, in the case of the Zonyl particles, the size of the interfacially-adsorbed particles (Fig. 5b and c; Fig. S2) is in the 1–10  $\mu\text{m}$  range which is far larger than the 0.2  $\mu\text{m}$  apparent in Fig. 2. Thus we conclude that the Zonyl particles remain aggregated to a significant extent even after our twin-screw extrusion process. An improvement in dispersion, e.g., by improving the extrusion operation, may have the beneficial effect of reducing bubble size of the Zonyl-containing foams without increasing the particle loading.

#### Failure of Foam Stabilization

The principle of particle-stabilization of foams is not based on specific chemical architectures such as branching or on improving melt strength, although incidental rheological changes may still occur due to the particles. Instead it is based on wettability considerations and interfacial effects of particles. Thus it is natural to ask whether the same strategy may be used with other plastics. As mentioned in the Introduction and detailed previously [24], a solid particle is likely to adsorb at the surface of a fluid only if the surface tension of the fluid exceeds the surface energy of the particle. Accordingly, particle-stabilization is most likely to be successful for plastics such as polyesters (e.g., the PLA used here, or the PS of Fig. S4), polyethers, polyamides, or unsaturated rubber compounds, all of which tend to have a high surface tension. In contrast, polymers such as saturated polyolefins, silicones, or fluorinated plastics inherently

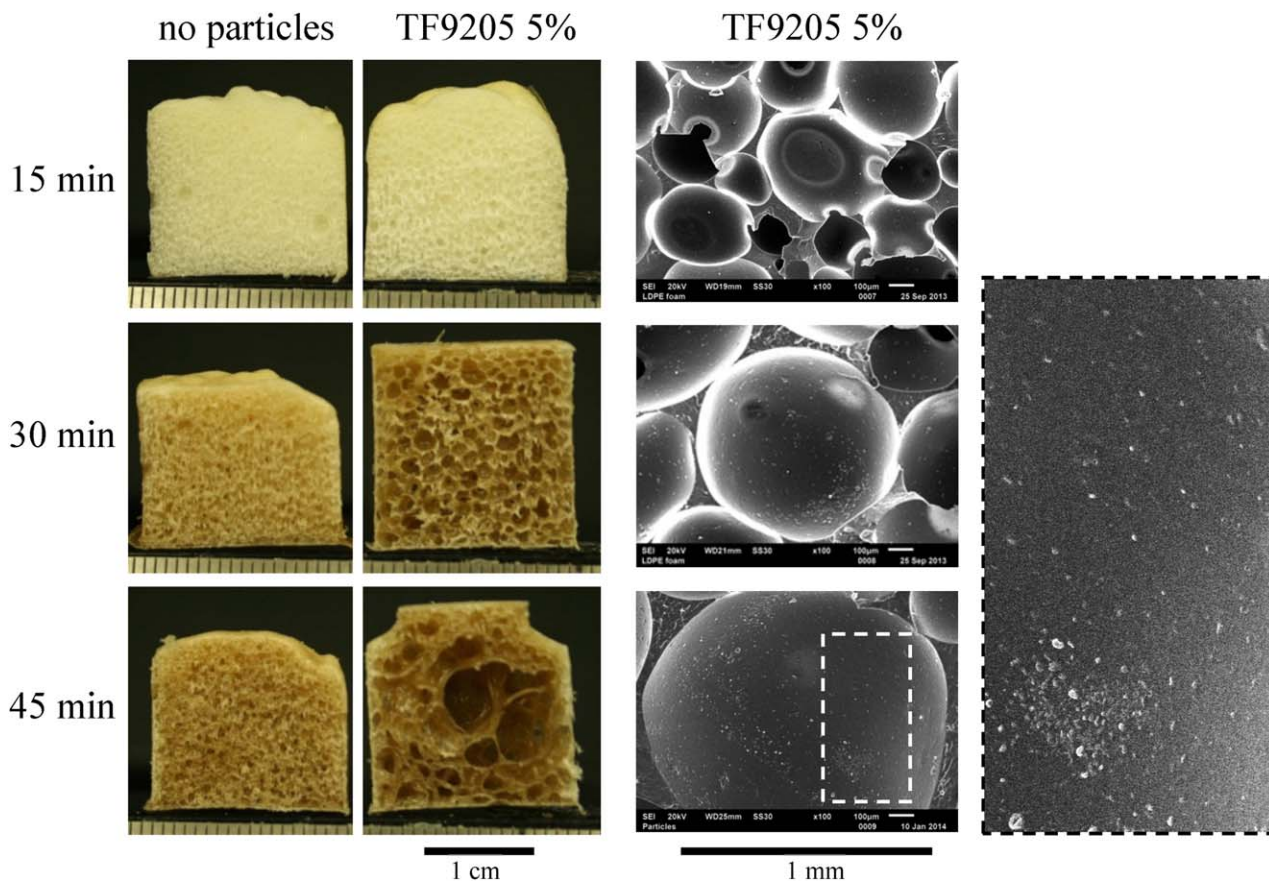


FIG. 7. Foaming experiments with LDPE with 1 g polymer in the foaming cell (corresponding to a nominal density of  $184 \text{ kg/m}^3$ ). Leftmost column is LDPE without added PTFE. The middle column and the SEM images on the right both correspond to 5% of the TF0205 particles. The image far right magnifies the dashed rectangle to show that while a few particles do appear at the interface, much of the interface remains free of particles. [Color figure can be viewed in the online issue, which is available at [wileyonlinelibrary.com](http://wileyonlinelibrary.com).]

have a low surface tension. Therefore particles are less likely to adsorb at their surface, and interfacial stabilization of foams is less likely to be successful.

To test this, experiments were conducted with three different polyolefins (Table 2), and all three show poor foam stabilization. Figure 7 shows one example: LDPE with 5 wt% TF9205 particles. Unlike PLA, the particle-free foam (left column of Fig. 7) does not collapse even after 45 minutes under molten conditions although an increase in cell size is apparent. Addition of PTFE particles does not retard this increase in cell size, in fact it accelerates coalescence, an effect that has been noted previously in aqueous foams or in polymer blends [31–33]. Similar results are seen for PP and polyolefin elastomer as well (Fig. S5 in the Electronic Supporting Information). In the case of PP, the particle-induced collapse of the foam is especially dramatic. Figure 7 and S3 support the idea that the idea of particle stabilization of foam is viable if the polymer being foamed has a relatively high surface energy.

## SUMMARY AND CONCLUDING REMARKS

In summary, this article shows that interfacially-active particles can be highly effective at stabilizing polymer foams. While proof-of-principle of this idea had already been established in our previous research [24], here we show that the same approach can be applied successfully using commercial

thermoplastic polymers foamed in a foaming operation that is similar to some of the ones used industrially. The experiments described here suggest the following mechanism for foam stabilization: particles adsorb at the interface during the foam expansion process, and then initial cell coalescence increases particle surface coverage sufficiently so that additional coalescence is arrested. This approach is most likely to be successful if the particles have low surface energy and the polymer melt being foamed has a high surface tension.

In this article, interfacial stabilization of foam is shown to overcome the limitations of poor melt strength, i.e., to produce stable foams from a polymer that was otherwise unfoamable. This paper also shows that the particle-stabilized foam is stable for extended periods under molten conditions, i.e., the strategy of interfacial stabilization can also extend the processing window within which foaming is possible. In particular, interfacial stabilization may prove useful in processes that require a foam to be held under molten conditions for extended periods, e.g., foaming of thick section or rotomolding, both of which involve slow cooling.

PTFE particles were used in this research because they have a low surface energy and hence are likely to adsorb at the air/molten polymer interface. However other particles with low surface energy may be equally effective: most notably hydrophobically modified fumed silicas or PP micropowders. These are much less expensive than PTFE and may offer other benefits,

e.g. fumed silica may also improve modulus and strength of the foams [34]. Thus, it is ironic that while PP itself is difficult to foam, PP particles may be an excellent foam stabilizer for other plastics.

## ACKNOWLEDGMENTS

The authors are grateful to Lanxess Inc. for supplying the blowing agent for foaming, and to DuPont and Dyneon for supplying the PTFE particles. They are grateful to Dr. Sushant Agarwal and Prof. Rakesh Gupta, West Virginia University, for extrusion-compounding the polypropylene foams of Supporting Information Fig. S5.

## NOMENCLATURE

CBA	Chemical blowing agent
PDMS	Polydimethylsiloxane
PIB	Polyisobutylene
PLA	Polylactic acid
PP	Polypropylene
PS	Polystyrene
PTFE	Polytetrafluoroethylene
SEM	Scanning electron microscopy

## REFERENCES

1. R.E. Drumright, P.R. Gruber, and D.E. Henton, *Adv. Mater.*, **12**, 1841 (2000).
2. K. Madhavan Nampoothiri, N.R. Nair, and R.P. John, *Biore-sour. Technol.*, **101**, 8493 (2010).
3. M. Nofar and C.B. Park, *Prog. Polym. Sci.*, **39**, 1721 (2014).
4. H. Tsuji and I. Fukui, *Polymer*, **44**, 2891 (2003).
5. R. Pop-Iliev, F. Liu, G. Liu, and C.B. Park, *Adv. Polym. Tech-nol.*, **22**, 280 (2003).
6. H.E. Naguib, C.B. Park, U. Panzer, and N. Reichelt, *Polym. Eng. Sci.*, **42**, 1481 (2002).
7. Y. Di, S. Iannace, E. Di Maio, and L. Nicolais, *Macromol. Mater. Eng.*, **290**, 1083 (2005).
8. C. Boissard, P.E. Bourban, C.J. Plummer, C. Neagu, and J.A.E. Manson, *J. Cell. Plast.*, **48**, 445 (2012).
9. A.J. Ro, S.J. Huang, and R.A. Weiss, *Polymer*, **50**, 1134 (2009).
10. A. Kulkarni, A. Lele, S. Sivaram, S. Velankar, and A. Chatterji, *Macromolecules*, in press, (2015). doi: 10.1021/acs.macromol.5b01854.
11. Y. Ema, M. Ikeya, and M. Okamoto, *Polymer*, **47**, 5350 (2006).
12. M.A. Paul, M. Alexandre, P. Degée, C. Henrist, A. Rulmont, and P. Dubois, *Polymer*, **44**, 443 (2003).
13. J.H. Chang, Y.U. An, and G.S. Sur, *J. Polym. Sci. Part B: Polym. Phys.*, **41**, 94 (2003).
14. S. Sinha Ray and M. Okamoto, *Prog. Polym. Sci.*, **28**, 1539 (2003).
15. Y. Di, S. Iannace, E.D. Maio, and L. Nicolais, *J. Polym. Sci. Part B: Polym. Phys.*, **43**, 689 (2005).
16. T.F. Tadros, *Chapter 8. Surfactants in Foams*, Wiley, Weinheim, 2005.
17. D.T. Wasan, in *Emulsions, Foams, and Thin Films*, K. L. Mittal and P. Kumar, Eds., Marcel Dekker, New York (2000).
18. R.J. Pugh, *Langmuir*, **23**, 7972 (2007).
19. B.P. Binks and T.S. Horozov, *Angew. Chem.*, **117**, 3788 (2005).
20. E. Dickinson, R. Ettelaie, T. Kostakis, and B.S. Murray, *Langmuir*, **20**, 8517 (2004).
21. U.T. Gonzenbach, A.R. Studart, E. Tervoort, and L.J. Gauckler, *Angew. Chem. Int. Ed. Engl.*, **45**, 3526 (2006).
22. S. Fujii, P.D. Iddon, A.J. Ryan, and S.P. Armes, *Langmuir*, **22**, 7512 (2006).
23. R.G. Alargova, D.S. Warhadpande, V.N. Paunov, and O.D. Velev, *Langmuir*, **20**, 10371 (2004).
24. P. Thareja, B.P. Ising, S.J. Kingston, and S.S. Velankar, *Macromol. Rapid Commun.*, **29**, 1329 (2008).
25. H. Otsuka, Y. Nagasaki, and K. Kataoka, *Adv. Drug Deliv. Rev.*, **64**, 246 (2012).
26. S. Wu, *J. Polym. Sci., C*, **34**, 19 (1971).
27. W. Rasband, Available at: <http://rsbweb.nih.gov/ij/>. Accessed September 27, 2015.
28. J. Pinto, E. Solorzano, M.A. Rodriguez-Perez, and J.A. de Saja, *J. Cell. Plast.*, **49**, 555 (2013).
29. M. Antunes, G. Gedler, and J.I. Velasco, *J. Cell. Plast.*, **49**, 259 (2013).
30. J. Lobos, S. Iasella and S. Velankar, Proceedings of the ANTEC meeting of the SPE (2014).
31. P. Thareja, K. Moritz, and S.S. Velankar, *Rheol. Acta*, **49**, 285 (2010).
32. P.R. Garrett, *Mode of Action of Antifoams*, Marcel Dekker, New York (1993).
33. S.P. Nagarkar and S.S. Velankar, *Soft Matter*, **8**, 8464 (2012).
34. J. Jobos and S.S. Velankar, *Journal of Cellular Plastics*, in press (2015), doi: 10.1177/0021955X14546015.